

Influence of Multiwall Carbon Nanotube on Physical Properties of Poly(ethylene 2,6-naphthalate) Nanocomposites

JUN YOUNG KIM, SEONG HUN KIM

Department of Fiber and Polymer Engineering, Center for the Advanced Functional Polymers, Hanyang University, Seoul 133-791, Korea

Received 3 July 2005; revised 27 September 2005; accepted 16 November 2005

DOI: 10.1002/polb.20728

Published online in Wiley InterScience (www.interscience.wiley.com).

ABSTRACT: Polymer nanocomposites consisting of multiwall carbon nanotube (MWCNT) and poly(ethylene 2,6-naphthalate) (PEN) were prepared by a melt blending process in a twin-screw extruder. The storage modulus (G') and loss modulus (G'') of the PEN/MWCNT nanocomposites increased with increasing frequency, and this increment being more significant at low frequency. The terminal zone slope of G' for the PEN/MWCNT nanocomposites decreased with increasing MWCNT content, and the nonterminal behavior of those was related to the dominant nanotube–nanotube interactions at higher MWCNT content, leading to the formation of the interconnected or network-like structures of MWCNT in the polymer nanocomposites. The decrease in the slope of the plot of $\log G'$ versus $\log G''$ for the PEN/MWCNT nanocomposites with increasing MWCNT content suggested the changes in the microstructures of the polymer nanocomposites by incorporating MWCNT. The incorporation of very small quantity of MWCNT significantly improved the mechanical properties of the PEN/MWCNT nanocomposites. © 2006 Wiley Periodicals, Inc. *J Polym Sci Part B: Polym Phys* 44: 1062–1071, 2006

Keywords: blending; carbon nanotube; nanocomposites; poly(ethylene 2,6-naphthalate); rheology

INTRODUCTION

As nanoscience and nanotechnology have advanced rapidly, extensive research and development have been performed on high performance polymeric nanomaterials for targeted applications in numerous industrial fields. Several attempts have been made to develop high performance polymer nanocomposites, with the benefit of nanotechnology, in fields ranging from the scientific to the industrial, including the incorporation of nanoscaled reinforcements into the polymer matrix. Carbon nanotubes (CNTs) have attracted

a great deal of interest as advanced reinforcements, since CNTs were discovered by Iijima in 1991.¹ Moreover, this discovery has created a high level of activity in materials research, leading to the practical realization of the extraordinary properties of CNTs, with their infinite number of possibilities for new materials.^{2–6}

As CNTs exhibit excellent electronic and remarkable physical properties, such as high aspect ratio and high mechanical strength, the fundamental research underlying the applications of CNTs suggests that they can be utilized as a promising reinforcement in new kinds of polymer nanocomposites.⁷ However, because of their high cost and limited availability, only a few practical applications in industrial fields have been realized to date. Furthermore, several studies on CNT-reinforced polymer nanocomposites have

Correspondence to: S. H. Kim (E-mail: kimsh@hanyang.ac.kr)

Journal of Polymer Science: Part B: Polymer Physics, Vol. 44, 1062–1071 (2006)
© 2006 Wiley Periodicals, Inc.

been conducted; however, their potential as nano-scaled reinforcements has not been fully realized.^{8–10}

One of the major challenges for high performance polymer nanocomposites is to optimize the processing operations of CNT-reinforced polymer nanocomposites with low costs. Three processing techniques have been commonly used to fabricate CNT-reinforced polymer nanocomposites: solution mixing, *in situ* polymerization, and melt compounding.^{11–16} Of these processing techniques, melt compounding has been accepted as the simplest and most effective method from an industrial perspective, because this process makes it possible to fabricate high performance nanocomposites at low cost, and also facilitates commercial scale-up. Furthermore, the combination of a very small quantity of expensive CNTs with cheap thermoplastic polymers may provide attractive possibilities for improving the mechanical properties of polymer nanocomposites.

The rheological behavior of polymer nanocomposites as a function of processing conditions is of great importance in polymer processing, particularly for the analysis and design of processing operations, as well as understanding structure-property relationships of polymer nanocomposites. In this regard, the rheological properties of CNT-reinforced polymer nanocomposites should be characterized both to realize the full potential of CNTs for application in thermoplastic matrix-based polymer nanocomposites and to optimize the processing conditions for achieving high performance polymer nanocomposites. However, the rheological behavior of CNT-reinforced conventional polyester nanocomposites has rarely been investigated to date, and most of the existing research involves CNT-filled polypropylene, polycarbonate (PC), and polyamide.^{16–18} Few reports can be found in the literature regarding the effect of CNTs on the rheological properties of polyester-based nanocomposites.

In this study, multiwall carbon nanotube (MWCNT)-reinforced poly(ethylene 2,6-naphthalate) (PEN) nanocomposites were prepared by a melt compounding in a twin-screw extruder to create advanced materials for possible practical applications in various industrial fields. To our knowledge, attempts to disperse MWCNT in the PEN matrix and to fabricate the PEN/MWCNT nanocomposites by melt compounding have not been previously investigated, and the study on the characterization of MWCNT and PEN nanocomposites have not yet been reported in the lit-

erature. The objective of this work is to characterize the effect of CNT on the physical properties of the PEN/MWCNT nanocomposites.

EXPERIMENTAL

The thermoplastic polymer used was PEN with an intrinsic viscosity of 0.97 dL/g, supplied by Hyo Sung Corp., Korea. The nanotubes used were MWCNT (degree of purity >95%) synthesized by a thermal chemical vapor deposition process, purchased from Iljin Nanotech, Korea. The MWCNT has the diameter of 10–40 nm and the length of 10–50 μm , implying that their aspect ratio reaches 1000. All materials were dried at 120 °C *in vacuo* for at least 24 h before use, to minimize the effects of moisture. MWCNT-reinforced PEN nanocomposites were prepared by a melt blending process in a Haake rheometer (Haake Technik GmbH, Germany) equipped with a twin-screw. The temperature of the heating zone, from the hopper to the die, was set to 280, 290, 295, and 285 °C, and the screw speed was fixed at 20 rpm. For the fabrication of the PEN/MWCNT nanocomposites, PEN was melt blended with the addition of various MWCNT content, specified as 0.1, 0.5, 1.0, and 2.0 wt % in the polymer matrix, respectively.

The rheological properties of PEN/MWCNT nanocomposites were measured at 285, 295, and 305 °C, covering the temperature processing windows of the polymer nanocomposites, with an ARES rheometer (Rheometric Scientific). The dynamic shear measurements were performed in oscillation mode and parallel-plate geometry with the plate diameter of 25 mm and the plate gap setting of ~ 1 mm, by applying a time-dependent strain, $\gamma(t) = \gamma_0 \sin(\omega t)$ and measuring resultant shear stress, $\gamma(t) = \gamma_0 [G' \sin(\omega t) + G'' \cos(\omega t)]$, where G' and G'' are storage and loss moduli, respectively. The frequency ranges were varied between 0.1 and 450 rad/s, and the strain amplitude was applied to be within the linear viscoelastic ranges.

The morphology of the PEN/MWCNT nanocomposites was observed using a JEOL 2000FX transmission electron microscope (TEM) and a field emission scanning electron microscopy (FE-SEM). The mechanical properties of the PEN/MWCNT nanocomposites were measured at room temperature using an Instron 4465 testing machine, according to the procedures in the ASTM D 638 standard. The gauge length and the crosshead speed were set

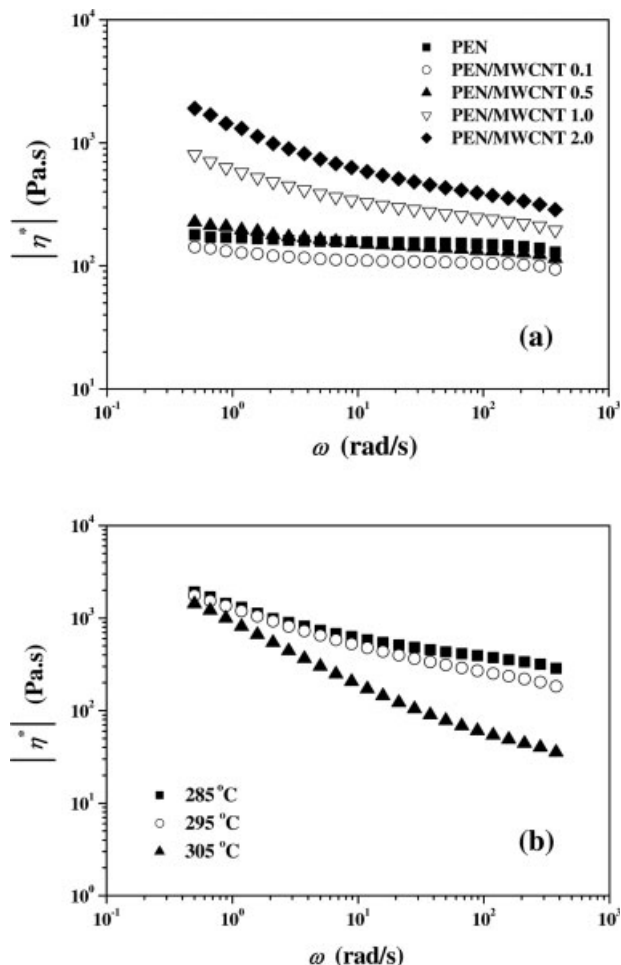


Figure 1. Variations of complex viscosity of (a) the PEN/MWCNT nanocomposites with the MWCNT content measured at 285 °C and (b) the PEN/MWCNT 2.0 nanocomposites at different temperatures, as a function of frequency.

to 20 mm and 10 mm/min, respectively. Thermogravimetric analysis of the PEN/MWCNT nanocomposites was performed with a TA Instrument SDF-2960 TGA over a temperature range of 30–800 °C, at a heating rate of 10 °C/min.

RESULTS AND DISCUSSION

The complex viscosities ($|\eta^*|$) of pure PEN and the PEN/MWCNT nanocomposites at 285 °C as a function of frequency are shown in Figure 1(a). The complex viscosities of PEN/MWCNT nanocomposites decreased with increasing frequency, indicating a non-Newtonian behavior over the frequency range investigated. The shear thinning behavior observed in the PEN/MWCNT nanocomposites may be attributed to the orientation of

the rigid molecular chains in the nanocomposites during the applied shear force. The effect of MWCNT on the $|\eta^*|$ of the PEN/MWCNT nanocomposites is more significant at low frequency compared with high frequency, and this effect was reduced with increasing frequency because of the strong shear thinning behavior induced by incorporating MWCNT. In addition, the irregular decrease in the $|\eta^*|$ with increasing frequency indicates pseudoplastic characteristics of the PEN/MWCNT nanocomposites because of random orientation and entangled molecules in this nanocomposite system. The frequency dependence of the $|\eta^*|$ of the PEN/MWCNT nanocomposites measured at various temperatures is shown in Figure 1(b). The $|\eta^*|$ of the PEN/MWCNT nanocomposites was decreased with increasing temperature. At low shear force region, the temperature had little effect on the $|\eta^*|$ of the PEN/MWCNT nanocomposites. However, the rheological properties of the PEN/MWCNT nanocomposites were affected by the temperature at high shear force region, and the $|\eta^*|$ significantly decreased with increasing temperature.

The shear thinning exponents (n) for the PEN/MWCNT nanocomposites can be obtained from the relationship of $|\eta^*| \approx \omega^n$,^{19,20} and their results are shown in Table 1. In this study, the shear thinning exponents of the PEN/MWCNT nanocomposites were estimated by fitting a straight line to the data at low frequency, because some curvature was observed in the plot of $\log|\eta^*|$ versus $\log \omega$. The n values of the PEN/MWCNT nanocomposites decreased with increasing MWCNT content, indicating that shear thinning behavior of the PEN/MWCNT nanocomposites significantly depended on MWCNT content. As shown in Table 1, the activation energy for the flow of the PEN/MWCNT nanocomposites increased with increasing MWCNT content. This

Table 1. Variations of Shear Thinning Exponent and Activation Energy of the PEN/MWCNT Nanocomposites with MWCNT Content

Materials	Shear Thinning Exponent (n)	Activation Energy, E_a (kJ/mol)
PEN	−0.13	59.40
PEN/MWCNT 0.1	−0.11	58.40
PEN/MWCNT 0.5	−0.17	66.52
PEN/MWCNT 1.0	−0.24	85.23
PEN/MWCNT 2.0	−0.34	87.23

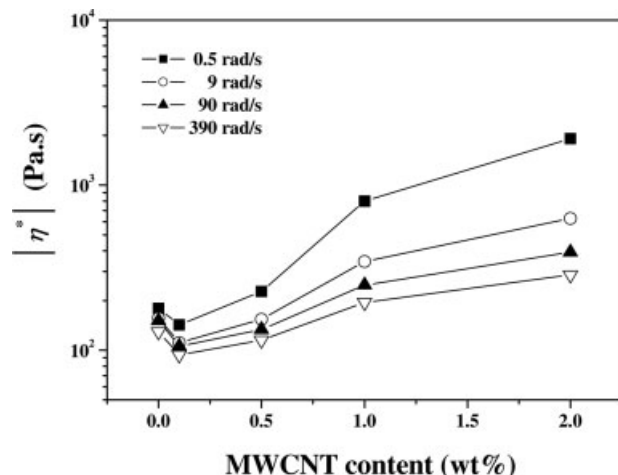


Figure 2. Variation of complex viscosities of PEN/MWCNT nanocomposites with MWCNT content at different frequencies.

result suggests that the incorporation of MWCNT leads to more rigid and stiffer polymer chains in the PEN/MWCNT nanocomposites, resulting in the increase in the activation energy for the flow process.

The variation of the $|\eta^*|$ of the PEN/MWCNT nanocomposites with the MWCNT content at different frequencies is shown in Figure 2. It can be seen that the $|\eta^*|$ of the PEN/MWCNT nanocomposites increased with increasing MWCNT content over the frequency ranges investigated. In addition, the extent of increase in the $|\eta^*|$ with increasing MWCNT content was more pronounced at low frequency compared with that at high frequency. Interestingly, it can be observed that the incorporation of a very small quantity (0.1 wt %) of MWCNT into the PEN matrix slightly decreased the complex viscosity of the PEN/MWCNT nanocomposites. This phenomenon may be attributed to the formation of the viscous surface layers around the dispersed nanotubes leading to an increase in the free volume in this nanocomposite system, making it easier for flow to occur.²¹ However, with further increase in MWCNT content, the $|\eta^*|$ of the PEN/MWCNT nanocomposites increased, and this may be attributed to the increase in physical interactions between the PEN matrix and the MWCNT with high aspect ratio and large surface area. The increase in the $|\eta^*|$ of the PEN/MWCNT nanocomposites with the MWCNT was closely related to the large increase in the storage modulus, which will be described in the following section.

The storage modulus (G') and loss modulus (G'') of the PEN/MWCNT nanocomposites as a function of frequency are shown in Figure 3. The values of G' and G'' of the PEN/MWCNT nanocomposites increased with increasing frequency and MWCNT content, this increment being more significant at low frequency. This rheological response is similar to the relaxation behavior of the typical filled-polymer composite systems.^{22,23} It is known that the polymer chains are fully relaxed and exhibit characteristic homopolymer-like terminal flow behavior, resulting in that the flow curves of polymers being expressed by the power law $G' \propto \omega^2$ and $G'' \propto \omega$.^{23–25} Krisnamoorti and Giannelis²⁶ reported that the slopes of $G'(\omega)$ and $G''(\omega)$ for polymer/layered silicate nanocomposite were much smaller than 2 and 1, respectively, which are the values expected for linear homodispersed polymer melts. They

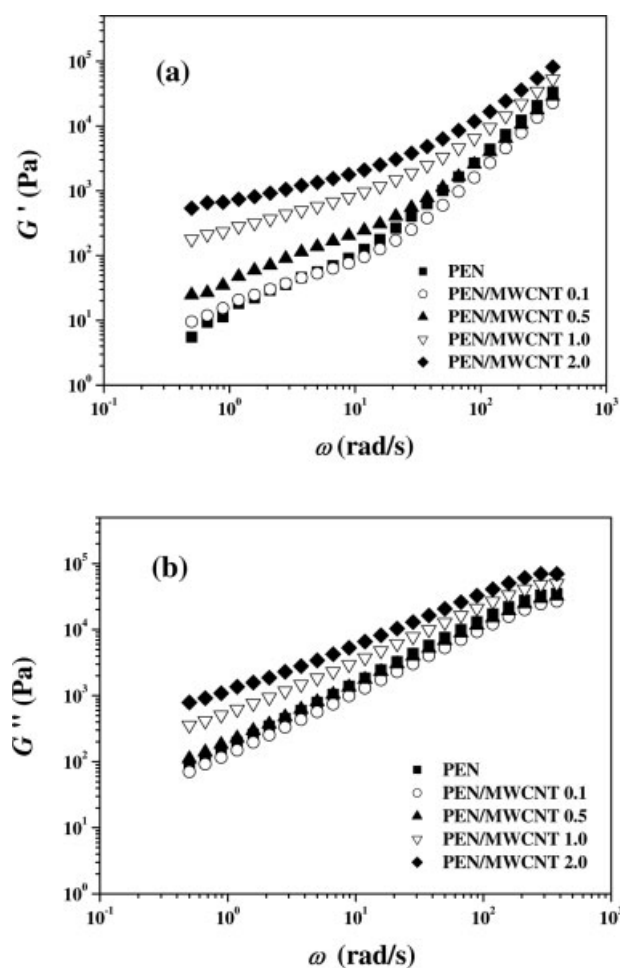


Figure 3. Variation of (a) storage modulus and (b) loss modulus of PEN/MWCNT nanocomposites with MWCNT content, as a function of frequency.

Table 2. Slopes of G' and G'' for PEN/MWCNT Nanocomposites

Materials	Slope of G'			Slope of G''		
	285 °C	295 °C	305 °C	285 °C	295 °C	305 °C
PEN	1.26	0.94	0.81	0.95	0.88	0.69
PEN/MWCNT 0.1	1.19	0.82	0.70	0.94	0.87	0.61
PEN/MWCNT 0.5	1.02	0.77	0.62	0.89	0.84	0.58
PEN/MWCNT 1.0	0.81	0.65	0.40	0.80	0.75	0.51
PEN/MWCNT 2.0	0.72	0.50	0.32	0.73	0.64	0.35

suggested that large deviations in the presence of a small quantity of layered silicate might be due to the formation of a network structure in the molten state. The slopes of the terminal zone of G' and G'' for the PEN/MWCNT nanocomposites are shown in Table 2, indicating the nonterminal behavior with the power-law dependence for G' and G'' of the PEN/MWCNT nanocomposites: the flow curves of the PEN/MWCNT nanocomposites can be expressed by a power law of $G' \propto \omega^{1.19 \sim 0.72}$ and $G'' \propto \omega^{0.95 \sim 0.73}$, respectively. Similar nonterminal low-frequency rheological behavior has been observed in ordered block copolymers and smectic liquid-crystalline small molecules.^{27,28} The decrease in the slope of G' for the PEN/MWCNT nanocomposites with increasing MWCNT content may be explained by the fact that the nanotube–nanotube interactions increased with increasing MWCNT content, and led to the formation of the interconnected or network-like structures of MWCNT in the polymer nanocomposites, resulting in the pseudo-solid-like behavior. In the PEN/MWCNT nanocomposites, the large deviations observed at high MWCNT content may be explained by the MWCNT agglomerates acted as large particles in terms of the dominant nanotube–nanotube interactions in the PEN/MWCNT nanocomposites matrix with increasing MWCNT content. For CNT/epoxy nanocomposite systems, it has been reported that the difference in the terminal zone slope was closely related to the internal structure of the CNT/epoxy nanocomposites, which is affected by particle–particle interaction of CNT in the polymer matrix.²⁹ In addition, the slopes of G' and G'' for the PEN/MWCNT nanocomposites decrease with increasing temperature, implying that the temperature can also affect the relaxation behavior of polymer chains in the PEN/MWCNT nanocomposites.

The variation of storage modulus (G') and loss modulus (G'') of the PEN/MWCNT nanocompo-

sites with the MWCNT content at different frequencies is shown in Figure 4. It can be seen that the incorporation of a very small quantity of the MWCNT (0.1 wt %) into the PEN matrix resulted in a decrease in the values of G' for the PEN/MWCNT nanocomposites over the frequency range investigated, except for the results mea-

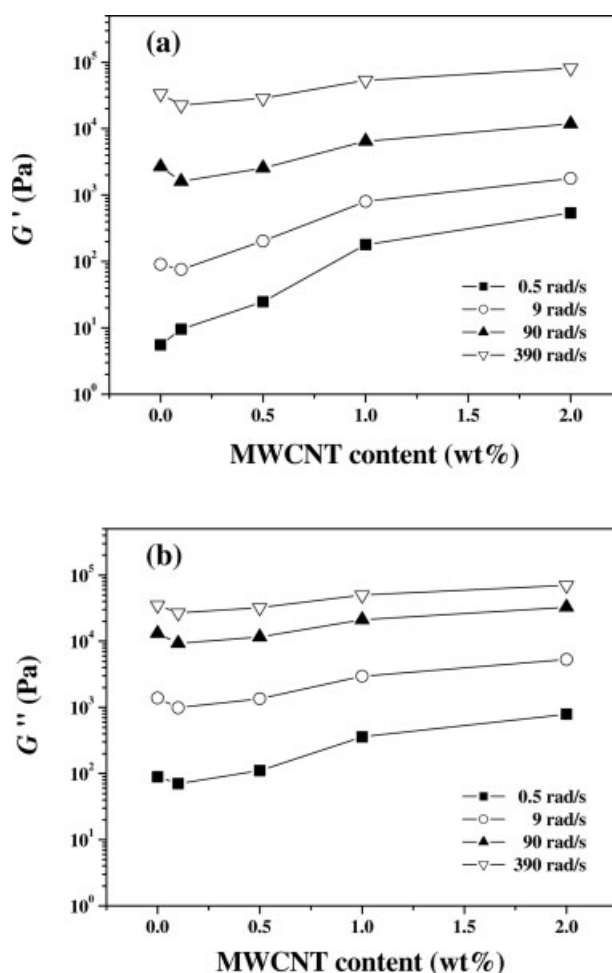


Figure 4. (a) Storage modulus and (b) loss modulus of PEN/MWCNT nanocomposites at different frequencies, as a function of MWCNT content.

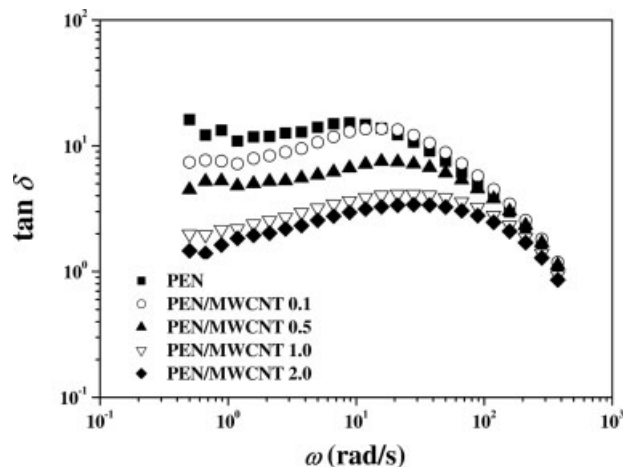


Figure 5. Variation of $\tan \delta$ with frequency for various PEN/MWCNT nanocomposites.

sured at very low frequency. This phenomenon was similar to the tendency observed in the variations of the complex viscosity for the PEN/MWCNT nanocomposites with the MWCNT content. As MWCNT content increased, the physical interactions between the nanotubes may lead to the formation of interconnected or network-like structure of the nanotubes in the polymer matrix.¹⁶ The extent of the increase in G' of the PEN/MWCNT nanocomposites is higher than that of G'' over the frequency range investigated. In addition, the storage modulus and loss modulus of the PEN/MWCNT nanocomposites were significantly improved relative to the PEN matrix, particularly at low frequency.

The variation of $\tan \delta$ with frequency for various PEN/MWCNT nanocomposites is shown in Figure 5. Shear deformation leads to the partial orientation of the molecules in polymer chains, resulting in the decrease in $\tan \delta$ of the PEN/MWCNT nanocomposites with increasing frequency. In addition, it can be seen that the loss tangent maximum shifted to higher frequency with increasing MWCNT content, implying the formation of dense network structures. Hsiao and coworkers³⁰ reported that for the polymer nanocomposites consisting of ethylene-propylene (EP) copolymers and polyhedral oligomeric silsesquioxane (POSS) molecules, the maximum in the $\tan \delta$ curves shifts toward a higher frequency as the POSS concentration was increased, indicating the densification of the physically crosslinked network in EP/POSS nanocomposites. Plots of the phase angle (δ) versus the absolute value of the complex modulus ($|G^*|$), which is known as the van Gorp-Palmen plot in the literature,^{31–33}

for the PEN/MWCNT nanocomposites measured at 285 °C, are shown in Figure 6. A significant change in the phase angle occurred on the incorporation of MWCNT, and the decrease in the phase angle with decreasing complex modulus indicates an increase in the elastic behavior. The PEN/MWCNT nanocomposites exhibited smaller δ values at lower complex modulus with increasing MWCNT content, implying that the incorporation of MWCNT enhanced the elasticity of the PEN/MWCNT nanocomposites.

As described in the previous section, the storage modulus and loss modulus of the PEN/MWCNT nanocomposites were higher than that of pure PEN, and increased with increasing MWCNT content. In general, the Cole–Cole plot, a logarithmic plot of G' versus G'' in dynamic rheology, provides a master curve with a slope of 2 for isotropic, and homogeneous polymer melts.³⁴ The extent of deviation from the slope of 2 has been commonly utilized in judging the heterogeneity of polymeric systems, because the slope of the plot of $\log G'$ versus $\log G''$ decreases as the heterogeneity increases. Plots of $\log G'$ versus $\log G''$ for the PEN/MWCNT nanocomposites with the MWCNT content are shown in Figure 7. The PEN/MWCNT nanocomposites do not provide a perfect single master curve, and exhibit shifts and changes of the slope of the plots with increasing MWCNT content. The slopes in the terminal regime of the PEN/MWCNT nanocomposites were less than 2, implying that the PEN/MWCNT nanocomposites underwent some chain conformational changes with the incorporation of

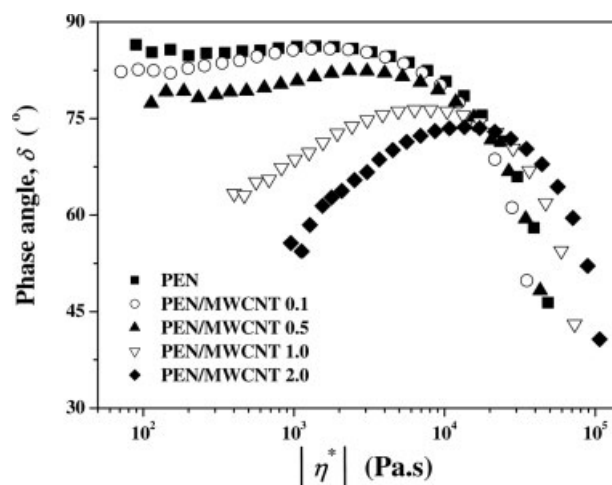


Figure 6. The plots of phase angle versus complex modulus of the PEN/MWCNT nanocomposites measured at 285 °C.

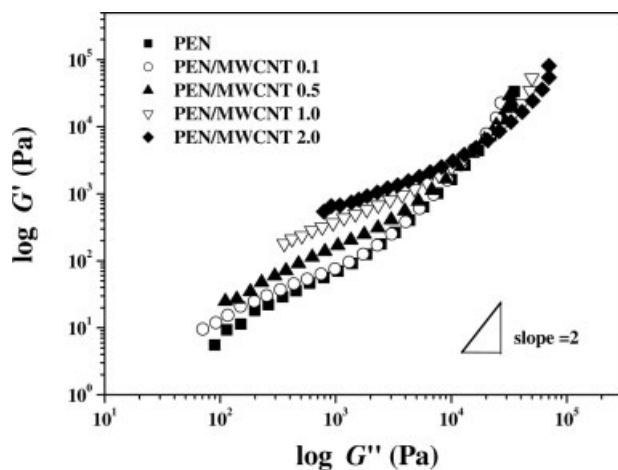


Figure 7. The plots of $\log G'$ versus $\log G''$ for the PEN/MWCNT nanocomposites with MWCNT content.

MWCNT. As shown in Figure 7, the storage modulus of the PEN/MWCNT nanocomposite at a given loss modulus increased with increasing MWCNT content. In addition, the slope of the plot of $\log G'$ versus $\log G''$ for the PEN/MWCNT nanocomposites decreased with increasing MWCNT content. Therefore, it can be deduced that incorporation of MWCNT has a significant effect on the microstructures for the PEN/MWCNT nanocomposites. For CNT/PC composites prepared by a melt compounding in a twin-screw extruder, Pötschke et al.¹⁶ suggested that the shift and the change in the slope of the plot of G' versus G'' for CNT/PC composites indicated a significant change in the microstructure of the polymer composites with the addition of CNTs. For a detailed analysis of this observation, our research currently in progress is aimed at characterizing the microstructure of CNT-reinforced PEN nanocomposites using small-angle X-ray scattering (SAXS) measurements.

The relaxation time (λ) of the PEN/MWCNT nanocomposites under dynamic shear in the polymeric systems that involved the pseudostructures can be calculated from the following equation³⁵:

$$J' = \frac{G'}{(|\eta^*|\omega)^2} = \frac{\lambda}{|\eta^*|} \quad (1)$$

where J' and η^* are the compliance and the complex viscosity, respectively. It is expected that the presence of some molecular order or the physical structure leads to a much longer relaxation time.³⁵ As shown in Figure 8, the relaxation time of the PEN/MWCNT nanocomposites decreased with increasing frequency. In addition, the relax-

ation time of the PEN/MWCNT nanocomposites increased with increasing MWCNT content. As MWCNT content increases, the nanotube–nanotube interactions will be dominant in the nanocomposite systems, and lead to the formation of interconnected structures of MWCNT in the PEN/MWCNT nanocomposites, which affects the relaxation behavior, and this effect being more pronounced at higher concentrations.

SEM microphotographs of pristine MWCNT and the PEN/MWCNT 2.0 nanocomposites are shown in Figure 9. MWCNT exhibits highly curved and random coiled features, which may be attributed to hydrogen bonding and van der Waals attractive interactions between CNTs.^{36,37} As shown in Figure 9(b), MWCNT were randomly dispersed in the PEN matrix, and the PEN/MWCNT nanocomposites exhibited the interconnected structure of MWCNT in the PEN matrix. The CNTs with small size, high aspect ratio, and large surface area are often subjected to self-agglomeration or bundle formation at higher concentration, and thus easily form interconnected or network-like structures in the molten polymer matrix. TEM images of the PEN/MWCNT nanocomposites are shown in Figure 10. It can be seen that MWCNT were randomly dispersed in the PEN matrix, with some entanglements or bundles of MWCNT. On a larger scale, however, the MWCNT were uniformly dispersed in the PEN matrix, despite some agglomerated MWCNT structures. In addition, MWCNT were randomly oriented and formed interconnecting structures.³⁸

The variation of tensile strength and tensile modulus of the PEN/MWCNT nanocomposites with the MWCNT content is shown in Figure 11.

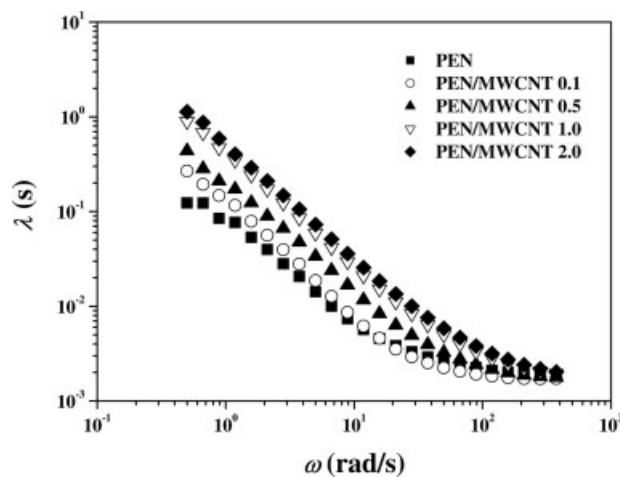
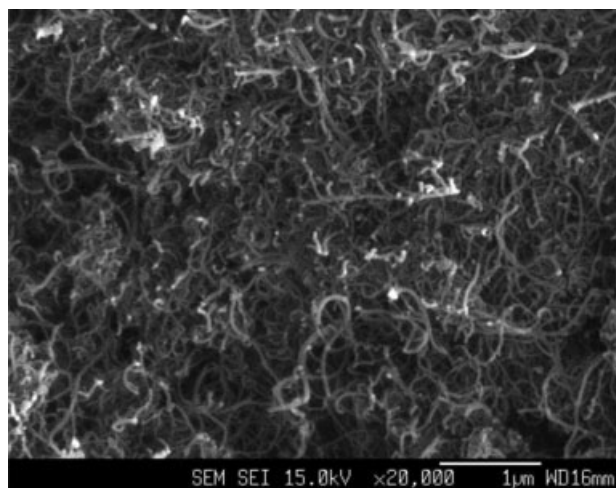
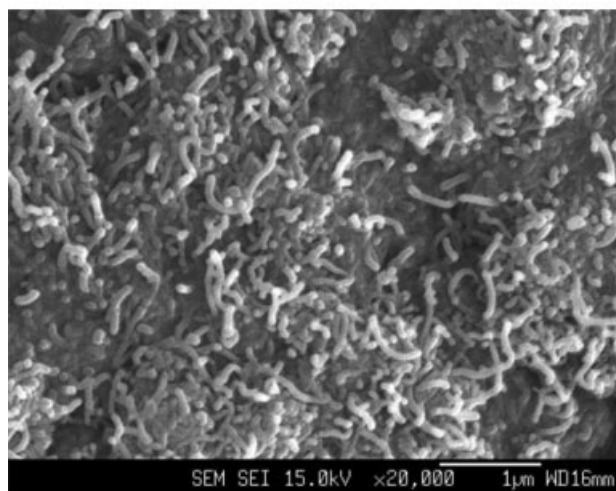


Figure 8. Variation of the relaxation time of the PEN/MWCNT nanocomposites with MWCNT content.



(a)



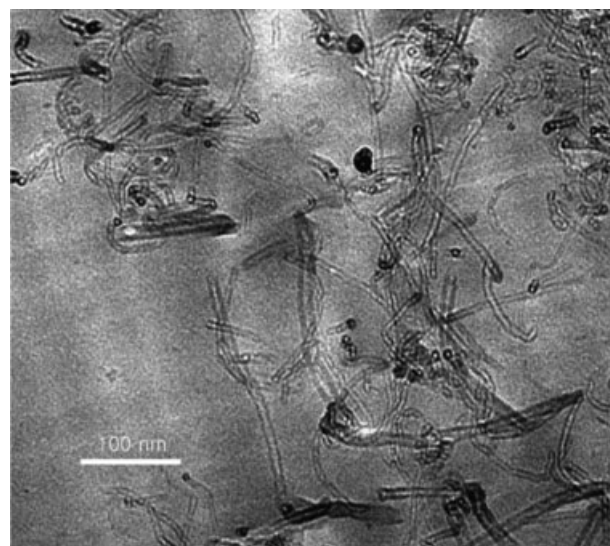
(b)

Figure 9. SEM microphotographs of (a) pristine MWCNT and (b) the PEN/MWCNT nanocomposites containing 2.0 wt % MWCNT.

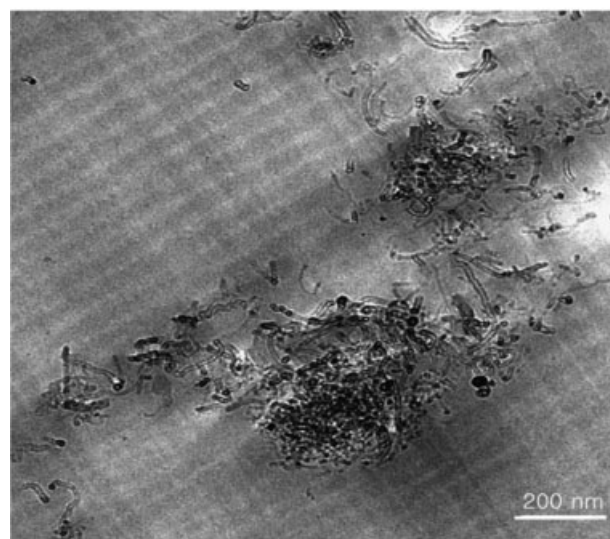
As MWCNT content increased, the tensile strength and tensile modulus of the PEN/MWCNT nanocomposites were improved due to the reinforcement effect of MWCNT with high aspect ratios, and this improvement being more significant at lower MWCNT content. However, CNTs often tend to bundle together because intrinsic van der Waals attraction between the individual tubes in combination with high aspect ratio and surface area of the nanotubes, leads to some agglomeration, and thus prevents efficient load transfer to the polymer matrix.^{3,36} At higher MWCNT content,

Journal of Polymer Science: Part B: Polymer Physics
DOI 10.1002/polb

less uniformly dispersed and more entangled bundles of MWCNT were formed in the PEN matrix, as shown in Figure 10(b), which may be the cause of the stress concentration phenomenon. As a result, the tensile strength of the PEN/MWCNT nanocomposites was not increased significantly at high MWCNT content, as expected, compared with that at low content, resulting



(a)



(b)

Figure 10. TEM microphotographs of PEN/MWCNT nanocomposites at (a) 0.1 wt % and (b) 2.0 wt % MWCNT content.

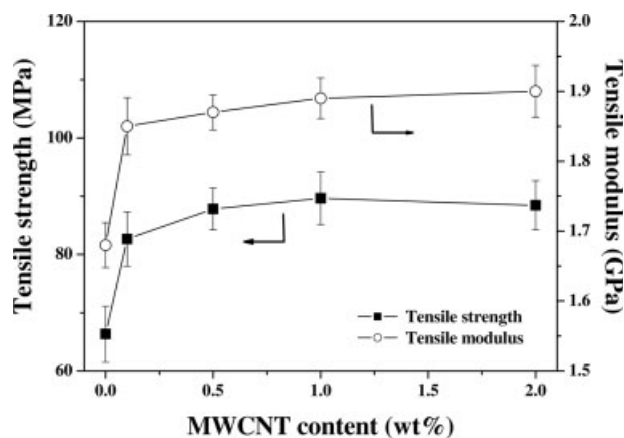


Figure 11. Variation of the tensile strength and tensile modulus of PEN/MWCNT nanocomposites with MWCNT content.

from some agglomerated structures of randomly dispersed MWCNT in the polymer nanocomposites. Therefore, to achieve further enhanced mechanical properties of the PEN/MWCNT nanocomposites, the improvement in both the dispersion of MWCNT in the PEN matrix and in the interfacial adhesion between the MWCNT and the PEN matrix through functionalization of CNTs should be required, and our current research is also aimed at that topic.

Thermal stability of polymer nanocomposites is one of the most important factors for polymer processing and targeted industrial application of polymers. Results from the TGA thermograms of the PEN/MWNT nanocomposites as a function of MWCNT content at a heating rate of 10 °C/min under a nitrogen atmosphere are shown in Table 3. The decomposition temperatures, including T_i , T_{10} , T_{60} , and T_{dm} , of the PEN/MWCNT nanocomposites increased with increasing MWCNT content, indicating that the thermal decomposition of the PEN/MWCNT nanocomposites was retarded by

incorporating MWCNT into the PEN matrix. In addition, the residual yields of the PEN/MWCNT nanocomposites increased with increasing MWCNT content, indicating that thermal decomposition of the polymer matrix was retarded in the PEN/MWCNT nanocomposites with higher residual yield. This result may be attributed to a physical barrier effect, resulting from the fact that MWCNT would prevent the transport of decomposition products in the polymer nanocomposites. Similar observations have been reported in that thermal stability of polypropylene/layered silicate nanocomposites was improved by a physical barrier effect, enhanced by ablative reassembling of the silicate layer.³⁹ Therefore, the TGA results demonstrate that the incorporation of a small quantity of MWCNT can significantly improve the thermal stability of the PEN/MWCNT nanocomposites.

CONCLUSIONS

The MWCNT-reinforced PEN nanocomposites were prepared by a melt blending process in a twin-screw extruder. The strong shear shinning behavior of the PEN/MWCNT nanocomposites resulted from the orientation of rigid molecular chains in the polymer nanocomposites. The extent of increase in the complex viscosity with increasing MWCNT content was more pronounced at low frequency compared with that at higher frequency. A gradual decrease in the terminal zone slope of G' for the PEN/MWCNT nanocomposites with increasing MWCNT content may be explained by the fact that the nanotube–nanotube interactions will be dominant at higher MWCNT content, and lead to the formation of the interconnected or network-like structures of MWCNT in the polymer nanocomposites. The

Table 3. Thermal Stability of PEN/MWCNT Nanocomposites with the MWCNT Content

Materials	T_i^a (°C)	T_{10}^b (°C)	T_{60}^b (°C)	T_{dm}^c (°C)	W_{800}^d (%)
PEN	389.2	412.4	447.4	436.8	14.8
PEN/MWCNT 0.5	390.6	417.2	457.1	438.7	22.7
PEN/MWCNT 1.0	397.7	420.4	461.4	439.8	26.9
PEN/MWCNT 2.0	398.2	422.2	467.9	440.9	30.3

^a Initial decomposition temperature in TGA at a heating rate of 10 °C/min.

^b Decomposition temperatures at 10% and 60% weight loss, respectively.

^c Decomposition temperature at the maximum decomposition rate.

^d Residual yield in TGA at 800 °C.

PEN/MWCNT nanocomposites exhibit smaller values of phase angle at lower complex modulus with increasing MWCNT content, implying that the elastic behavior of the PEN/MWCNT was enhanced by incorporating MWCNT. The decrease in the slope of the plot of $\log G'$ versus $\log G''$ for the PEN/MWCNT nanocomposites with increasing MWCNT content suggests that the microstructures of the PEN/MWCNT nanocomposites is affected by incorporating MWCNT. The mechanical properties of the PEN/MWCNT nanocomposites significantly improved with even very small quantity of MWCNT.

This research was supported by Korea Science and Engineering Foundation directed Engineering Research Center, Center for the Advanced Functional Polymers (Project No. R11-1997-044-07,022-0).

REFERENCES AND NOTES

- Iijima, S. *Nature* 1991, 354, 56.
- Iijima, S.; Ichihashi, T. *Nature* 1993, 363, 603.
- Dresselhaus, M. S.; Dresselhaus, G.; Avouris, P. H. *Carbon Nanotubes: Synthesis, Structure, Properties, and Applications*; Springer: Berlin, 2001.
- Wong, E. W.; Sheehan, P. E.; Lieber, C. M. *Science* 1997, 277, 1971.
- Yao, Z.; Zhu, C. C.; Cheng, M.; Liu, J. *Comput Mater Sci* 2001, 22, 180.
- Yu, M. F.; Files, B. S.; Arepalli, S.; Ruoff, R. S. *Phys Rev Lett* 2000, 84, 5552.
- Antonucci, V.; Hsiao, K. T.; Advani, S. G. In *Advanced Polymeric Materials: Structure Property Relationships*; Shonaike, G. O.; Advani, S. G., Eds.; CRC Press: New York, 2003; Ch. 11, pp 397–437.
- Schadler, L. S.; Giannaris, S. C.; Ajayan, P. M. *Appl Phys Lett* 1998, 73, 3842.
- Wong, M.; Paramsothy, M.; Xu, X. J.; Ren, Y.; Li, S.; Liao, K. *Polymer* 2003, 44, 7757.
- Frankland, S. J. V.; Harik, V. M. *Surf Sci* 2003, 505, L103.
- Haggenmuller, R.; Conmas, R. H. H.; Rinzler, A. G.; Fischer, J. E.; Winey, K. I. *Chem Phys Lett* 2000, 330, 219.
- Jia, Z. J.; Wang, Z. Y.; Liang, J.; Wei, B. Q.; Wu, D. H. *Mater Sci Eng A* 1999, 271, 395.
- Jin, J. X.; Pramoda, K. P.; Goh, S. H.; Xu, Q. *Mater Res Bull* 2002, 37, 271.
- Kim, J. Y.; Park, H. S.; Kim, S. H. *Polymer* 2006, in press.
- Kim, J. Y.; Park, H. S.; Kim, S. H. *J. Appl Polym Sci*, submitted for publication (2005).
- Pötschke, P.; Fornes, T. D.; Paul, D. R. *Polymer* 2002, 43, 3247.
- Seo, M. K.; Park, S. J. *Chem Phys Lett* 2004, 395, 44.
- Bhattacharyya, A. R.; Pötschke, P.; Abdel-Goad, M.; Fischer, D. *Chem Phys Lett* 2004, 392, 28.
- Abdel-Goad, M.; Pötschke, P. J. *Non-Newtonian Fluid Mech* 2005, 128, 2.
- Wagener, R.; Reisinger, T. J. G. *Polymer* 2003, 44, 7513.
- Kulichikhin, V. G.; Shumskii, V. F.; Semakov, A. V. In *Rheology and Processing of Liquid Crystal Polymers*; Acierno, D.; Collyer, A. A., Eds.; Chapman & Hall: New York, 1996; Ch. 5, pp 135–184.
- Enikolopyan, N. S.; Fridman, M. L.; Stalnova, I. U.; Popov, V. L. *Adv Polym Sci* 1990, 96, 1.
- Krishnamoorti, R.; Vaia, R. A.; Giannelis, E. P. *Chem Mater* 1996, 8, 1728.
- Ferry, J. *Viscoelastic Properties of Polymers*; Wiley: New York, 1980.
- Okamoto, M. In *Encyclopedia of Nanoscience and Nanotechnology*; Nalwa, H. S., Ed.; American Scientific Publisher: Los Angeles, 2004; Vol. 8, pp 791–843.
- Krisnamoorti, R.; Giannelis, E. P. *Macromolecules* 1997, 30, 4097.
- Rosedalev, J. H.; Bates, F. S. *Macromolecules* 1990, 23, 3239.
- Larson, R. G.; Winey, K. I.; Patel, S. S.; Watanabe, H.; Bruinsma, R. *Rheol Acta* 1993, 32, 245.
- Song, Y. S.; Youn, J. R. *Carbon* 2005, 43, 1378.
- Fu, B. X.; Gelfer, M. Y.; Hsiao, B. S.; Phillips, S.; Viers, B.; Blanski, R.; Ruth, P. *Polymer* 2003, 44, 1499.
- Van Gulp, M.; Palmen, J. *Rheol Bull* 1998, 67, 5.
- Trinkle, S.; Friedrich, C. *Rheol Acta* 2002, 41, 103.
- Honerkamp, J.; Weese, J. *Rheol Acta* 1993, 32, 57.
- Ottenbrite, R. M.; Utracki, L. A.; Inoue, S. *Current Topics in Polymer Science*; Carl Hanser: Munich, 1991.
- Wissbrun, K. F.; Griffin, A. C. J. *Polym Sci Polym Phys Ed* 1982, 20, 1895.
- Ebbesen, T. *Carbon Nanotubes: Preparation and Properties*; CRC press: New York, 1997.
- Li, S. N.; Li, Z. M.; Yang, M. B.; Hu, Z. Q.; Xu, X. B.; Huang, R. *Mater Lett* 2004, 58, 3967.
- Park, S. J.; Kim, J. S. *Carbon* 2001, 39, 2011.
- Zanetti, M.; Camino, G.; Reichert, P.; Mulhaupt, R. *Macromol Rapid Commun* 2001, 22, 176.